

# Microfibre–nanowire hybrid structure for energy scavenging

Yong Qin<sup>1\*</sup>, Xudong Wang<sup>1\*</sup> & Zhong Lin Wang<sup>1</sup>

A self-powering nanosystem that harvests its operating energy from the environment is an attractive proposition for sensing, personal electronics and defence technologies<sup>1</sup>. This is in principle feasible for nanodevices owing to their extremely low power consumption<sup>2–5</sup>. Solar, thermal and mechanical (wind, friction, body movement) energies are common and may be scavenged from the environment, but the type of energy source to be chosen has to be decided on the basis of specific applications. Military sensing/surveillance node placement, for example, may involve difficult-to-reach locations, may need to be hidden, and may be in environments that are dusty, rainy, dark and/or in deep forest. In a moving vehicle or aeroplane, harvesting energy from a rotating tyre or wind blowing on the body is a possible choice to power wireless devices implanted in the surface of the vehicle. Nanowire nanogenerators built on hard substrates were demonstrated for harvesting local mechanical energy produced by high-frequency ultrasonic waves<sup>6,7</sup>. To harvest the energy from vibration or disturbance originating from footsteps, heartbeats, ambient noise and air flow, it is important to explore innovative technologies that work at low frequencies (such as <10 Hz) and that are based on flexible soft materials. Here we present a simple, low-cost approach that converts low-frequency vibration/friction energy into electricity using piezoelectric zinc oxide nanowires grown radially around textile fibres. By entangling two fibres and brushing the nanowires rooted on them with respect to each other, mechanical energy is converted into electricity owing to a coupled piezoelectric–semiconductor process<sup>8,9</sup>. This work establishes a methodology for scavenging light-wind energy and body-movement energy using fabrics.

The fibres used in our experiments were Kevlar 129 fibres, which have high strength, modulus, toughness and thermal stability. ZnO nanowires were then grown radially on the fibre surface using a hydrothermal approach<sup>10</sup>. A typical scanning electron microscopy (SEM) image of a Kevlar fibre covered by ZnO nanowires is shown in Fig. 1a. Along the entire length of the fibre, ZnO nanowires grew radially and exhibited a very uniform coverage and well preserved cylindrical shape. Some splits in the nanowire arrays can be identified (Fig. 1b), which were produced owing to the growth-induced surface tension in the seeding layer. All of the ZnO nanowires are single crystalline, and have a hexagonal cross-section with a diameter in the range ~50–200 nm and a typical length of ~3.5 μm. Their top and side surfaces are smooth and clean, indicating that they are able to form the reliable metal–semiconductor junctions needed for the nanowire nanogenerators. The space between the nanowires is of the order of a few hundred nanometres, which is large enough for them to be bent to generate the piezoelectric potential<sup>11</sup>. The nanowires' tips are separated from each other owing to their small tilting angles (<±10°), but their bottom ends are tightly connected (Fig. 1b inset).

As a result, a continuous ZnO film at the nanowires' roots served as a common electrode for signal output. Previous experiments showed that AFM (atomic force microscope) manipulation of a solution-grown ZnO nanowire can give up to 45 mV output voltage<sup>12</sup>.

To maintain the high flexibility of the fibre after growing a crystalline film and nanowires, a surface coating strategy was introduced to improve the mechanical performance of the fibre and the binding of nanowires. Two layers of tetraethoxysilane (TEOS) were infiltrated—one above and one below the ZnO seed layer—as binding agents (Fig. 1c). The Si–O bonds in TEOS are highly reactive with the OH<sup>−</sup> groups on the ZnO surface<sup>13</sup>, and its organic chains firmly bind to the body of the aromatic polyamide fibre. As a result, the ZnO seed layer and the fibre core were tightly bound with each other by a thin layer of TEOS. Furthermore, since TEOS could easily form cross-linked chains, the nanowires were firmly bundled and bound together at their roots and fixed on the ZnO seeding layer,

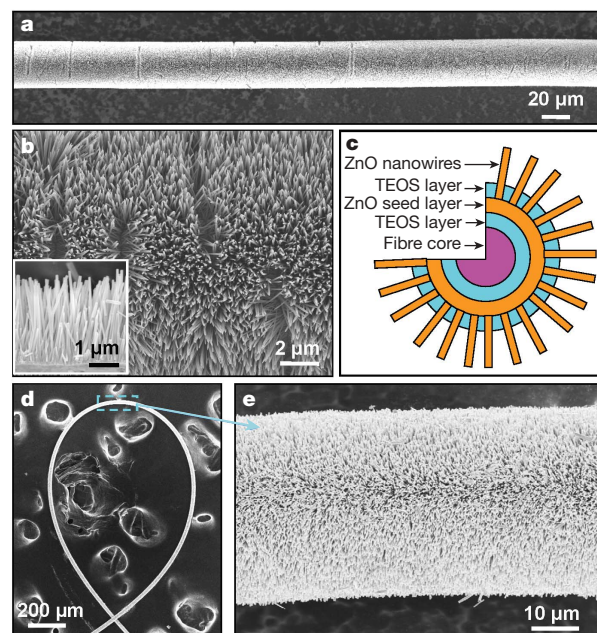


**Figure 1 | Kevlar fibres coated with ZnO nanowires.** **a**, An SEM image of a Kevlar fibre covered with ZnO nanowire arrays along the radial direction. **b**, Higher magnification SEM image and a cross-section image (inset) of the fibre, showing the distribution of nanowires. **c**, Diagram showing the cross-sectional structure of the TEOS-enhanced fibre, designed for improved mechanical performance. **d**, SEM image of a looped fibre, showing the flexibility and strong binding of the nanowire layer. **e**, Enlarged section of the looped fibre, showing the distribution of the ZnO nanowires at the bending area.

<sup>1</sup>School of Materials Science and Engineering, Georgia Institute of Technology, Atlanta, Georgia 30332-0245, USA.

\*These authors contributed equally to this work.

successfully preventing them from scratching/stripping off during mechanical brushing/sliding. Even when the fibre was looped into a circle of  $\sim 1$  mm in diameter, no cracks, loose pieces or peel-offs were observed in the ZnO nanowire coating layer (Fig. 1d). At the bending area, the radially aligned morphology of the ZnO nanowires was also very well preserved (Fig. 1e), clearly demonstrating its toughness under mechanical deformation and bending.

In order to demonstrate the power generation ability of the ZnO-nanowire-covered fibres, a double-fibre model system was designed (Fig. 2a). Two fibres, one coated with a 300-nm-thick gold layer and the other as-grown, were entangled to form the core for power generation. The relative brushing between the two fibres was simulated by pulling/releasing the string using an external rotor with a controlled frequency. The gold-coated fibre was connected to the external circuit as the nanogenerator's output cathode. The pulling force

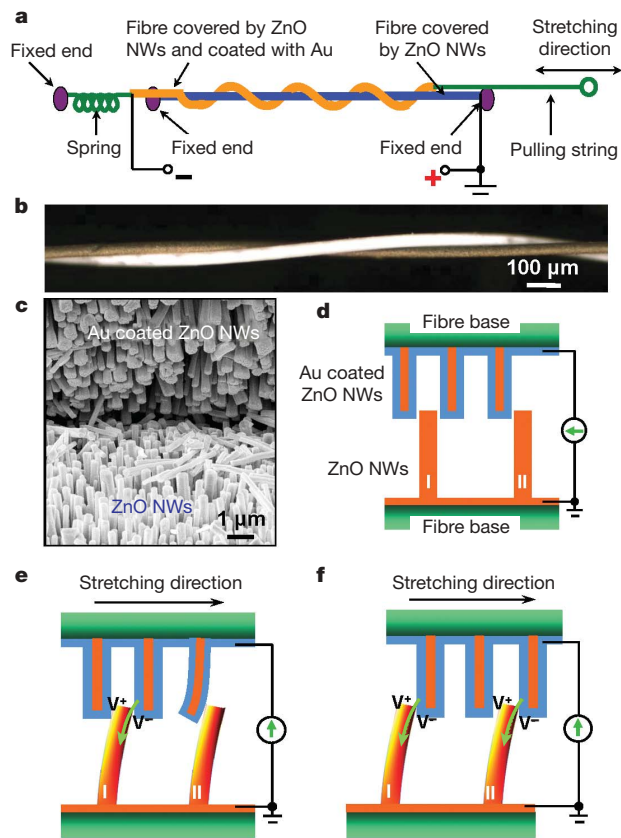


**Figure 2 | Design and electricity-generating mechanism of the fibre-based nanogenerator driven by a low-frequency, external pulling force.**

**a**, Schematic experimental set-up of the fibre-based nanogenerator. **b**, An optical micrograph of a pair of entangled fibres, one of which is coated with Au (in darker contrast). **c**, SEM image at the 'teeth-to-teeth' interface of two fibres covered by nanowires (NWs), with the top one coated with Au. The Au-coated nanowires at the top serve as the conductive 'tips' that deflect/bend the nanowires at the bottom. **d**, Schematic illustration of the teeth-to-teeth contact between the two fibres covered by nanowires. **e**, The piezoelectric potential created across nanowires I and II under the pulling of the top fibre by an external force. The side with positive piezoelectric potential does not allow the flow of current owing to the existence of a reverse-biased Schottky barrier. Once the nanowire is pushed to bend far enough to reach the other Au-coated nanowire, electrons in the external circuit will be driven to flow through the uncoated nanowire due to the forward-biased Schottky barrier at the interface. **f**, When the top fibre is further pulled, the Au-coated nanowires may scrub across the uncoated nanowires. Once the two types of nanowires are in final contact, at the last moment, the interface is a forward biased Schottky, resulting in further output of electric current, as indicated by arrowheads. The output current is the sum of all the contributions from all of the nanowires, while the output voltage is determined by one nanowire.

ensured a good contact between the two fibres, as shown by an optical microscopy image (Fig. 2b).

In this design, the gold-coated ZnO nanowires acted as an array of scanning metal tips that deflected the ZnO nanowires rooted at the other fibre; a coupled piezoelectric and semiconducting property resulted in a process of charge creation and accumulation and charge release<sup>8,9</sup>. The gold coating completely covered the ZnO nanowires and formed a continuous layer along the entire fibre. A successful coating was confirmed by its metallic  $I$ - $V$  characteristic (Supplementary Fig. 1). Once the two fibres were firmly entangled together, some of the gold-coated nanowires penetrated slightly into the spaces between the uncoated nanowires rooted at the other fibre, as shown by the interface image in Fig. 2c. Thus, when there was a relative sliding/deflection between them, the bending of the uncoated ZnO nanowires produced a piezoelectric potential across their width, and the Au-coated nanowires acted as the 'zigzag' electrode (as for the DC nanogenerator<sup>6</sup>) for collecting and transporting the charges.

Figure 2d-f illustrates the charge generation mechanism of the fibre nanogenerator. Like the deflection of a nanowire by an AFM tip<sup>8</sup>, when the top fibre move to the right, for example, the gold-coated nanowires bend the uncoated ZnO nanowires to right (for simplicity of description, we assume that the gold-coated nanowires are much stiffer and suffer little bending). Piezoelectric potential is thus generated across the uncoated nanowire owing to its piezoelectric property, with the stretched surface positive ( $V^+$ ) and the compressed surface negative ( $V^-$ )<sup>8</sup>. The positive-potential side has a reverse-biased Schottky contact with the gold (see the  $I$ - $V$  curve in Supplementary Fig. 2) that prevents the flow of current, while the negative-potential side has a forward-biased Schottky contact with the gold that allows the current to flow from the gold to the nanowire. As the density of the nanowires is high (Fig. 1b), it is very likely that a bent nanowire rooted at the uncoated fibre touches the backside of another gold-coated nanowire after subjecting to bending (such as nanowire I in Fig. 2e). In this case, the negative-potential surface of the ZnO nanowire contacts the gold layer, so the Schottky barrier at the interface<sup>14</sup> is forward biased, resulting in a current flowing from the gold layer into the ZnO nanowire. Then, when the top fibre keeps moving further towards the right (Fig. 2f), the gold-coated nanowires scan across the ZnO nanowires' tips and reach their negatively charged sides (nanowires I and II in Fig. 2f). Therefore, more current will be released through the forward-biased Schottky barriers (Fig. 2f). This means that the currents from all of the nanowires will add up constructively regardless of their deflection directions, even in the same cycle of pulling.

The output voltage is defined by the characteristic of one nanowire, and the sign of the voltage does not change in response to the deflection configuration of the nanowire owing to the rectifying effect of the Schottky barrier at the Au-ZnO interface. The same effect is expected if the top fibre is driven to the left. Owing to the similar mechanical properties of the top and bottom nanowires, the gold-coated nanowires could also be possibly bent by the nanowires rooted at the uncoated fibre, but this does not affect the mechanism presented in Fig. 2. For the gold-coated fibre, all of the nanowires are completely covered by a thick gold layer, and they can be considered as an equal-potential electrode (Supplementary Fig. 1) connected to the external measurement circuit. Thus, the role played by these ZnO nanowires was only to act as a template for supporting the Au coating, and no piezoelectric charges will be preserved inside the gold-coated nanowires.

The short-circuit current ( $I_{sc}$ ) and open-circuit voltage ( $V_{oc}$ ) were measured to characterize the performance of the fibre nanogenerators. The pulling and releasing of the gold-coated fibre was accomplished by a motor at a controlled frequency. The resulting current signals detected at 80 r.p.m. (revolutions per minute; 60 r.p.m. = 1 Hz) are shown in Fig. 3a. A 'switching polarity' testing method was applied during the entire measurement to rule out system artefacts. When the current meter was forward-connected to the

nanogenerator, which means that the positive and negative probes were connected to the positive and negative electrodes of the nanogenerator as defined in Fig. 2a, respectively,  $\sim 5$  pA positive current pulses were detected at each pulling-releasing cycle (blue curve in Fig. 3a). Negative current pulses with the same amplitude were received (pink curve in Fig. 3a) when the current meter was reverse-connected, with its positive and negative probes connected to the negative and positive electrodes of the nanogenerator, respectively. The small output current ( $\sim 5$  pA) is attributed mainly to the large loss in the fibre due to an extremely large inner resistance ( $R_i \approx 250$  M $\Omega$ ; see Supplementary Fig. 3). This large inner resistance of the fibre-based nanogenerator is probably due to cracks in the ZnO seed layer directly adjacent to the fibre that are caused by the structural incompatibility and large difference in thermal expansion coefficients. Reducing  $R_i$  of the fibre nanogenerator is an effective way to improve its power output efficiency, which is demonstrated in Fig. 4c.

The inverted output current signals confirmed that the current was indeed originated from the fibre nanogenerator. The shapes of the positive and negative current pulse are enlarged and shown in Fig. 3c and d, respectively, from which a double-peak feature is clearly observed for each cycle of pulling the fibre.

Open-circuit voltage was also measured by the switching polarity method. Corresponding positive and negative voltage signals were received when the voltage meter was forward- and reverse-connected to the fibre nanogenerator, respectively (Fig. 3b). The amplitude of the voltage signal in this case was  $\sim 1$ –3 mV (see also Supplementary Fig. 4). As for the current signal, a double-peak feature was also observed in both positive and negative voltage signals (Fig. 3e and f).

The double peaks in the output signal (Fig. 3c–f) are related to the cycle motion of the fibre. When the fibre was pulled to the right-hand-side during stretching and then retracted back by the spring

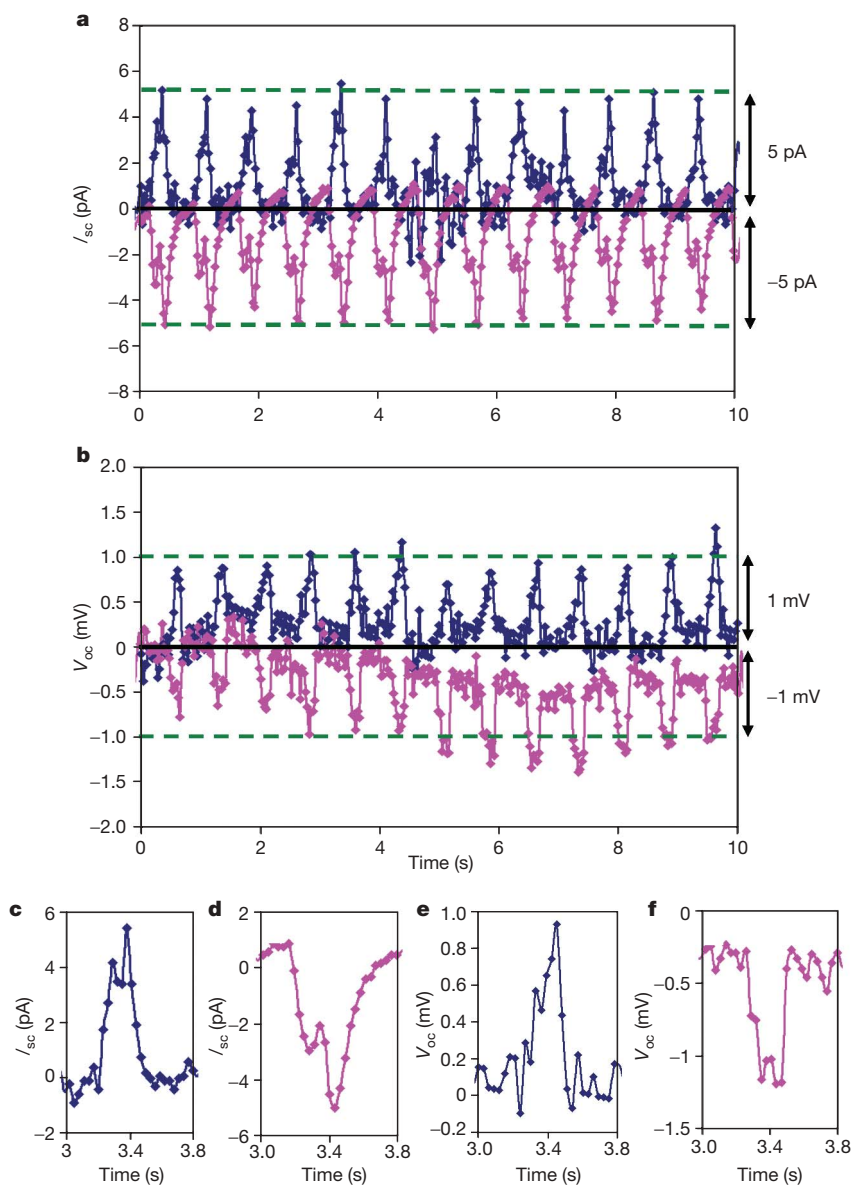


**Figure 3 | Electric output of a double-fibre nanogenerator.** **a**, The short-circuit output current ( $I_{sc}$ ) and **b**, the open-circuit output voltage ( $V_{oc}$ ) of a double-fibre nanogenerator measured by applying an external pulling force at a motor speed of 80 r.p.m. When the measurement circuit was forward-connected to the nanogenerator, which means that the positive and negative probes were connected to the positive and negative output electrodes of the

nanogenerator, respectively, the output signals are represented by a pink curve. By reversing the polarity of the connection of the nanogenerator output electrodes, the output signals are presented by the blue curve. **c**, **d**, Magnified output current and **e**, **f**, output voltage for a single cycle of the fibre pulling. The background introduced by the measurement circuit was removed in the displayed plots.



when released, the mechanism illustrated in Fig. 2 remained the same. Although the two moving directions were opposite, the currents generated flowed in the same direction, and a delay of  $\sim 0.2$  s of one with respect to the other produced double peaks in the resultant output current and voltage. This is a general phenomenon that existed in every output pulse regardless of its polarity. A slight difference in the magnitude of the double peaks may be related to the speed at which the fibre was pulled and retracted.

To exclude the possible contribution made by friction-induced electrostatic charges during the relative sliding/brushing of the two fibres, we have used two fibres both with or without Au coating. For the fibres both without Au coating, no output electric signal was detected (Supplementary Fig. 5a): and for the fibres both with Au coating, no output electricity was detected either (Supplementary Fig. 5b). This means that the observed signal is unrelated to friction induced charging/discharging.

The fibre nanogenerator also exhibited good performance over a range of frequencies. Short-circuit current was measured while the speed of the driving motor was varied from 80 to 240 r.p.m. (Supplementary Fig. 6). The current density decreased almost linearly with the increase of frequency (Supplementary Fig. 7). Owing to the relatively high friction force between the entangled fibres, it takes time for the fibre to recover to its original shape after releasing. As the frequency increases, the time intervals left for the spring to retract the fibre became shorter and shorter, thus, the fibre was not fully recovered to its static shape before the next pulling started, resulting in less travelling distance for the fibre and the smaller electric output.

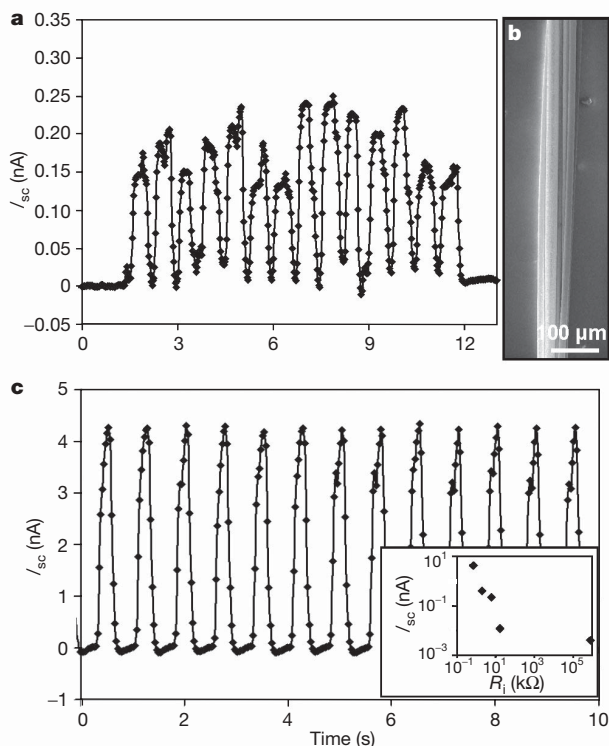


**Figure 4 | Output improvements.** **a**, The short-circuit output current ( $I_{sc}$ ) of the multi-fibre nanogenerator operated at 80 r.p.m. A broadening in the output current peaks is observed due to the unsynchronized movement among the fibres. **b**, SEM image of the multi-fibre nanogenerator composed of six ZnO-nanowire-coated fibres, three of which were gold-coated. This shows the possibility of using a bundle of nanowires as a yarn for enhancing the output current. **c**, Enhancement of output current by reducing the inner resistance ( $R_i$ ) of the nanogenerator. By coating the surface of the fibre first with a conductive layer, then depositing ZnO seeds, the inner resistance of the nanogenerator was reduced by orders of magnitude. The background introduced by the measurement circuit was removed in the displayed plots.

After demonstrating the electricity generation principle, a few approaches were investigated to increase the output power and prototype integration. To simulate a practical fabric made of yarn, a single yarn made of 6 fibres was tested; three fibres were covered with nanowires and coated with Au, and three were only covered with nanowires. All of the gold-coated fibres were movable in the testing (Fig. 4b). At a motor speed of 80 r.p.m., an average current of  $\sim 0.2$  nA was achieved (Fig. 4a), which is  $\sim 30$ – $50$  times larger than the output signal from a single-fibre nanogenerator: this is due to the substantially increased surface contact area among the fibres. The width of each pulse was broadened, apparently due to the unsynchronized movement and a relative delay in outputting current among the fibres.

Reducing the inner resistance of the fibre and the nanowires was found to be effective for enhancing the output current. By depositing a conductive layer directly onto the fibre before depositing the ZnO seeds, the inner resistance of the nanogenerator was reduced from  $\sim 1$  G $\Omega$  to  $\sim 1$  k $\Omega$ ; thus the output current  $I_{sc}$  of a double-fibre nanogenerator was increased from  $\sim 4$  pA to  $\sim 4$  nA (Fig. 4c). The current  $I_{sc}$  is approximately inversely proportional to the inner resistance of the nanogenerator (inset in Fig. 4c). This study shows an effective approach for increasing the output current. In addition, by connecting nanogenerators in series and parallel, the output voltage and current, respectively, can be increased as well<sup>7</sup>.

Life-time testing of the fibre nanogenerator was performed at a motor speed of 80 r.p.m. for 1 min and 30 min of continuous operation. The ZnO nanowire array was robust and stood up well to the relative brushing between the two fibres, and no broken area was observed after 30 min of continuous sliding/brushing (Supplementary Fig. 8a, b). An SEM image recorded from the contact area shows that, just after 1 min operation, a small fraction of ZnO nanowires had been stripped off the fibres. These nanowires were either stuck in the gaps between gold-coated nanowires or laid on the surface (Supplementary Fig. 8c). However, after 30 min of continuous brushing, the fraction of stripped-off nanowires showed no significant increase (Supplementary Fig. 8d). This suggests that the nanowires that were stripped after the first 1 min (Supplementary Fig. 8c) were probably the loose ones in the arrays, which would be stripped off anyway at any stage of the experiment, but the remaining nanowires were bonded well to the substrate. This experiment further confirms that the TEOS infiltration had effectively improved the mechanical toughness and stability of the ZnO nanowires and the life-time of the fibre nanogenerator.

The textile-fibre-based nanogenerator has demonstrated the following innovative advances in comparison to the DC nanogenerators reported previously<sup>6</sup>. First, using ZnO nanowires grown on fibres, it is possible to fabricate flexible, foldable, wearable and robust power sources in any shape (such as a 'power shirt'). Second, the output electricity can be dramatically enhanced using a bundle of fibres as a yarn, which is the basic unit for fabrics. The optimum output power density from textile fabrics can be estimated on the basis of the data we have reported, and an output density of 20–80 mW per square metre of fabric is expected (see Supplementary Information). Third, the nanogenerator operates at low frequency, in the range of conventional mechanical vibration, footsteps and heartbeats, greatly expanding the application range of nanogenerators. Last, as the ZnO nanowire arrays were grown using chemical synthesis at 80 °C on a curved substrate, we believe that our method should be applicable to growth on any substrate, so the fields in which the nanogenerators can be applied and integrated may be greatly expanded. The near-term goal is to optimize the structure and design in order to improve the efficiency and total output power.

## METHODS SUMMARY

The ZnO nanowires were grown radially around Kevlar 129 fibres using a hydrothermal approach. The as-grown ZnO nanowires were then chemically bonded to the fibre surface as well as to each other by coating with TEOS. The

double-fibre nanogenerator was assembled by entangling a fibre covered with as-grown nanowires around the other fibre covered with gold-coated nanowires. By fixing the two ends of one fibre, and sliding the other fibre back and forth, a relative brushing motion between the two fibres produces output current due to coupled piezoelectric–semiconducting properties. Short circuit current and open circuit voltage were recorded when the two fibres were slid with respect to each other.

**Full Methods** and any associated references are available in the online version of the paper at [www.nature.com/nature](http://www.nature.com/nature).

**Received 10 October; accepted 13 December 2007.**

- Paradiso, J. A. & Starner, T. Energy scavenging for mobile and wireless electronics. *Pervasive Comput.* **4**, 18–27 (2005).
- Li, Y., Qian, F., Xiang, J. & Lieber, C. M. Nanowire electronic and optoelectronic devices. *Mater. Today* **9**, 18–27 (2006).
- Tian, B. *et al.* Coaxial silicon nanowires as solar cells and nanoelectronic power sources. *Nature* **449**, 885–890 (2007).
- Javey, A., Guo, J., Wang, Q., Lundstrom, M. & Dai, H. J. Ballistic carbon nanotube field-effect transistors. *Nature* **424**, 654–657 (2003).
- Chen, J. *et al.* Bright infrared emission from electrically induced excitons in carbon nanotubes. *Science* **310**, 1171–1174 (2005).
- Wang, X. D., Song, J. H., Liu, J. & Wang, Z. L. Direct-current nanogenerator driven by ultrasonic waves. *Science* **316**, 102–105 (2007).
- Wang, X. D., Liu, J., Song, J. H. & Wang, Z. L. Integrated nanogenerators in biofluid. *Nano Lett.* **7**, 2475–2479 (2007).
- Wang, Z. L. & Song, J. H. Piezoelectric nanogenerators based on zinc oxide nanowire arrays. *Science* **312**, 242–246 (2006).
- Song, J. H., Zhou, J. & Wang, Z. L. Piezoelectric and semiconducting coupled power generating process of a single ZnO belt/wire: A technology for harvesting electricity from the environment. *Nano Lett.* **6**, 1656–1662 (2006).
- Hsu, J. W. R. *et al.* Directed spatial organization of zinc oxide nanorods. *Nano Lett.* **5**, 83–86 (2005).
- Gao, Y. F. & Wang, Z. L. Electrostatic potential in a bent piezoelectric nanowire: The fundamental theory of nanogenerator and nanopiezotronics. *Nano Lett.* **7**, 2499–2505 (2007).
- Gao, P. X., Song, J. H., Liu, J. & Wang, Z. L. Nanowire piezoelectric nanogenerators on plastic substrates as flexible power sources for nanodevices. *Adv. Mater.* **19**, 67–72 (2007).
- Wu, Y. L., Tok, A. I. Y., Boey, F. Y. C., Zeng, X. T. & Zhang, X. H. Surface modification of ZnO nanocrystals. *Appl. Surf. Sci.* **253**, 5473–5479 (2007).
- Liu, J. *et al.* Carrier density and Schottky barrier on the performance of DC nanogenerator. *Nano Lett.* **8**, 328–332 (2008).

**Supplementary Information** is linked to the online version of the paper at [www.nature.com/nature](http://www.nature.com/nature).

**Acknowledgements** This research was supported by the DOE, the NSF, and Emory-Georgia Tech CCNE funded by the NIH.

**Author Contributions** Z.L.W., X.W. and Y.Q. designed the experiments; Y.Q. and X.W. performed the experiments; and Z.L.W. and X.W. analysed the data and wrote the paper. All authors discussed the results and commented on the manuscript.

**Author Information** Reprints and permissions information is available at [www.nature.com/reprints](http://www.nature.com/reprints). Correspondence and requests for materials should be addressed to Z.L.W. ([zlwang@gatech.edu](mailto:zlwang@gatech.edu)).

## METHODS

**Fabrication of ZnO-nanowire-coated fibre.** Kevlar 129 fibres were used, 14.9  $\mu\text{m}$  in diameter. First, the fibres were cleaned in acetone then ethanol under sonication for 5 min each. A 100-nm-thick ZnO seed layer was uniformly coated around the fibre using magnetron sputtering. ZnO nanowires were then grown radially on the fibre surface via a hydrothermal approach by immersing the fibres in the reactant solution at 80 °C. The reactant solution was prepared by dissolving 0.1878 g of  $\text{Zn}(\text{NO}_3)_2 \cdot 6\text{H}_2\text{O}$  and 0.0881 g of hexamethylenetetramine in 250 ml deionized water at room temperature. The concentration of each in the solution was 0.025  $\text{mol l}^{-1}$ . After 12-h ageing in the solution, the fibres turned white, indicating that they were covered by dense ZnO nanowires. Finally, they were rinsed with deionized water several times and baked at 150 °C for 1 h. The as-synthesized ZnO-nanowire-coated fibres were immersed in 99.9% TEOS for 2–3 min. Because the as-deposited ZnO seed layer usually has some cracks owing to its incompatibility with the fibre, capillary force can attract TEOS through the cracks to reach the interface between the ZnO seed layer and the fibre as well as the roots of the nanowires. Thus, two layers of TEOS, above and below the ZnO seed layer, were formed.

**Assembly of double-fibre nanogenerator.** A typical double-fibre nanogenerator was assembled using two 3-cm-long ZnO-nanowire-coated fibres, one coated with Au and one as-grown. The Au layer was coated by a DC sputtering system. During the sputtering, the fibre was fixed on the stage at one end and its body was left free-standing. Therefore, a fairly uniform Au coating was achieved along entire fibre by rotating the sample stage. Generally, the thickness of the Au coating was  $300 \pm 20$  nm, which was read by a quartz thickness monitor inside the sputtering system. In assembling the double-fibre nanogenerator, both ends of the as-grown ZnO nanowire fibre were fixed on a glass substrate, with one end grounded and electrically connected to an external measurement circuit as the nanogenerator's output anode. One end of the gold-coated fibre was attached to a small spring, which was affixed to the substrate; the other end was attached to a pulling string so that it could freely move back and forth. The gold-coated fibre was electrically connected to the external circuit as the nanogenerator's output cathode. The effective length of the fibre nanogenerator was 4–5 mm and typically contained nine entangled cycles, where each cycle was  $\sim 500$   $\mu\text{m}$  in length.

**Testing of fibre nanogenerator.** The double-fibre nanogenerator was fixed on a stationary stage with the movable gold-coated fibre attached to a pulling bar. The pulling bar was driven by a speed control motor with an extrusion on its spin axis, which transferred its rotary motion into a back-and-forth motion of the pulling bar at a chosen frequency. During each rotation, the gold-coated fibre first moved to the pulling direction when the pulling bar was lifted up; then was retracted back to its original position by the spring attached to the other end. The back-and-forth brushing movement between the two fibres was thus achieved at a controlled frequency. The current signal was monitored by a DL 1211 preamplifier (DL Instruments). The voltage signal was detected by a SR560 low noise preamplifier (Stanford Research Systems, Inc.). Both signals were converted through a BNC-2120 analogue-to-digital converter (National Instruments) and recorded by a computer. The resistance of the fibre nanogenerator was determined by analysing the  $I$ - $V$  characteristic using a DS345 30 MHz synthesized function generator (Stanford Research Systems) as the voltage source. The entire system was placed inside a Faraday cage to minimize environmental interference. The measurements were performed at room temperature without monitoring or controlling humidity.